Increasing the transverse aperture of the AP2-Debuncher injection region

F. Bieniosek
30 June 1998

Overview.

This report describes the changes required to increase the transverse aperture of the AP2-Debuncher injection region. It is based on the vacuum chamber dimensions and MAD output provided by M. Church [Ref. 1]. Using an Excel spreadsheet, and a simple optics model, I recalculated the optics of the injection region. I used POISSON calculations of the magnetic field in the quadrupoles to determine the extent of the good field regions. The calculations were used to develop a strategy to relocate the aperture restrictions in the injection area, and to bump the circulating and injected beams around them. The aperture upgrade is divided into two parts. The first part is to be applied with the existing septum. It is relatively simple and provides good horizontal and vertical aperture through the injection region. The second part requires a new septum. It improves the horizontal and vertical apertures to 40 π by further moving D4Q5 and other optical elements. Antiproton yield into the Debuncher, as estimated by MCLENS, is projected to increase by up to 70%.

Proposal.

Here are the required beampipe modifications. These modifications will be substantiated in the text below.

1. Install vertical and horizontal motion control on D4Q8 so that this quad can be moved remotely by ±5 mm in either direction. This requires new bellows also.
2. Offset D4Q3 upward by 2.7 mm, or, preferably, install vertical motion control on this magnet also.
3. Offset the beampipe and flanges between SEM403 and D4Q4 upward by 4 mm.
4. Offset the septum downstream end downward by about 7 mm from its current location. Install a motor on the septum stand for remote vertical adjustment, by ±5 mm.
5. Offset the upstream end of the septum downward by 6 mm from its current location.
6. Offset D4Q5 upward by 3.1 mm, downstream by 6.0 cm, and tilt to face AP2 by 8 mrad. It may be necessary to move or shorten the pile of shielding bricks between D4Q5 and the injection septum.
7. Build a new beampipe for injected beam through D4Q5 that fills the available space between pole faces.

The injection region is likely to be a major aperture limitation. The above modifications should increase the vertical aperture through the injection region from its present approximately 21 π mm mrad to 33 π if the kicker can produce a deflection of 6.4 mrad. The horizontal aperture on the vertical centerline of the beam is projected to increase from 26 π to 31 π. If the injection region is the sole aperture limitation, yield into the Debuncher

should increase by about 35%, based on a calculation using MCLENS, using the theoretical existing apertures of 26 x 21 π.

To obtain an aperture of 40 π the following is required.

8. To realize the full aperture increase, a new septum with a wider horizontal aperture and thinner septum gap will need to be made. It will relocated downstream by up to 30 cm. Horizontal beta function will be somewhat larger than in its current location. Thus it will be necessary to increase the horizontal width of the new septum to 47 mm. Septum and power supply requirements are detailed in Table 4.
9. To realize the full aperture increase in the vertical dimension, the kicker must produce a deflection of at least 6.6 mrad, and the septum must be reduced by at least 1 mm.
10. Further magnet moves are required, as listed in Table 3 below. They may be updated after the results from Solution 1 are obtained.

If the full 40 π aperture is achieved in both planes, yield into the Debuncher is projected to increase an additional 25%.

Optical elements in the injection region.

There are several elements of the Debuncher that play an important role in injection of beam from AP2. The injection process uses off-axis deflection at large quad D4Q5 to help combine the injected and circulating beams. The septum further deflects the injected beam toward the circulating beam. The injected beam passes well off axis at D4Q4 before reaching the kicker, and D4Q3 also provides some steering. Finally the kicker deflects the injected beam to the position of the circulating beam. For details of placement and dimensions of the vacuum chamber, see Ref.1.

D4Q5.

Fig. 1 shows the field gradient (i.e., the quadrupole component) calculated by POISSON for large distances from the axis, using the dimensions of a large quad lamination. At these distances the iron in the laminations is close to saturation. The shape of the gradient plot at large distances depends to some extent on the amount of saturation; these calculations are for the nominal operating field. These are of course 2-D calculations, and do not take into account fringe fields. But the end packs of these magnets were carefully designed to be neutral, so end effects should not be large. Also shown is the injected beam in its current position (centered at about 148 mm off axis). It is located at the extreme upper edge of the good field region. Portions of a centered 40-π vertical emittance beam sample the fall-off of the field gradient at large vertical position. Vertical dispersion for injected beam at this position is about 0.13 m, according to P138. A 2% off-momentum beam thus has an additional excursion of 2.6 mm. Incidentally, I have been unable to find any field measurements for this magnet at the time of manufacture at positions higher than 5.5" = 140 mm. In fact, the injected beam passes very close to the top of the beam pipe where the pipe touches the bus bar for the magnet.

The horizontal aperture available in the gap between the pole faces is indicated in Fig. 2. This plot is based on the horizontal beta function at D4Q5, and the known lamination dimensions, allowing 2 mm horizontal thickness for the vacuum wall. Fig. 2 shows the existing beam positions upstream and downstream, and the existing vacuum chamber. The existing vacuum chamber limits horizontal aperture to 26 π. This can be improved somewhat by using a triangular-shaped chamber that closely approximates the pole face

(Fig. 3). More improvement can be obtained by moving the beam downward; an aperture of 40 π corresponds to a vertical height on the magnet of 127 mm. This requires a vertical offset of 20 mm from the beam's current position to provide 40 π horizontal aperture in the center of the beam. Cutting the pole face to provide a larger horizontal aperture as suggested in Ref. 1 severely affects the quadrupole component of the field.

The strategy for redesigning the optics for a move of this magnitude is based on a combination of three translations of D4Q5. No redesign of the magnet is required.
(a) An upward vertical translation of the magnet lowers the beam position on the pole face. The vertical translation introduces a vertical kick in the circulating beam, which must be corrected elsewhere in the injection region. Vertical kicks in the injected beam are similarly corrected by adjustments in the septum strength and other elements in the region.
(b) A longitudinal translation of the magnet downstream lowers the beam position on the pole face because the vertical height of the beam is lower at a downstream location. The disadvantage of such a move is that the lattice functions of the circulating beam are affected. Longitudinal translation should be kept small. It is limited to 12 cm in this proposal. Such a translation lowers the effective height of the beam at D4Q5 by 7.5 mm.
(c) A tilt of the magnet to face the injected beam lowers the beam position on the pole face as the face seen by the injected beam is raised up vertically. If the magnet is tilted such as to pivot about its midplane, the effect on circulating beam is small. The projected tilt angles are in the range of 10-20 mrad. Such a tilt raises the front face of the magnet 4-8 mm. This angle is somewhat larger than the natural angles of divergence/convergence of circulating beam in the Debuncher, which are typically 4 mrad or less. Therefore the effects of such a tilt on the circulating beam should be studied in detail.

First order terms.

The standard equations for a beam trajectory in a defocusing quadrupole are

$$y(z) = y_1 \cosh\sqrt{\kappa}z + y_1' / \sqrt{\kappa} \sinh\sqrt{\kappa}z$$
$$y'(z) = y_1 \sqrt{\kappa} \sinh\sqrt{\kappa}z + y_1' \cosh\sqrt{\kappa}z$$

where the quadrupole strength is $\sqrt{\kappa} = (B'/B\rho)^{1/2} = 0.5741$ m^{-1} for D4Q5, according to the TURTLE model [Ref. 2], which is in agreement with the MAD model. The effective magnet length ℓ is 0.823 m. Note that the factor z in the equation strictly refers to beam path length in the magnet, not the longitudinal length of the magnet. If the magnet is tilted an angle θ with respect to the Debuncher centerline, the trajectory through the magnet may

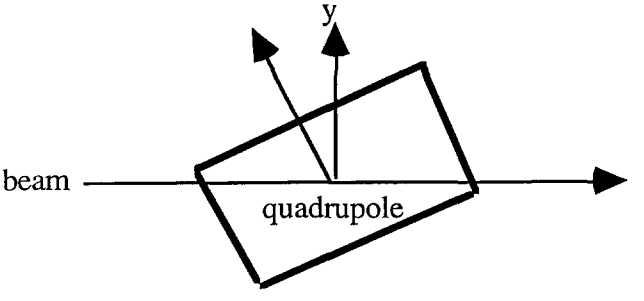

be translated to a new coordinate ξ, where

$$\xi = y\cos\theta - z\sin\theta$$
$$\xi' = y'\cos\theta - \sin\theta$$

which may be approximated to 1 part in 10^4, by the simplifying assumption $\cos\theta = 1$. The beam is followed through the magnet by converting from y to ξ at the entrance of the magnet and back to y at the exit of the magnet.

The expressions for the change in beam deflection caused by tilting a quadrupole magnet about its midplane are

$$\Delta y(\ell) = \sin\theta\left\{\frac{\ell}{2}\left(\cosh\sqrt{\kappa}\ell + 1\right) - \frac{1}{\sqrt{\kappa}}\sinh\sqrt{\kappa}\ell\right\}$$
$$\Delta y'(\ell) = \sin\theta\left\{\frac{\ell}{2}\sqrt{\kappa}\sinh\sqrt{\kappa}\ell + 1 - \cosh\sqrt{\kappa}\ell\right\}$$

Agreement between the first order approximation represented by the equations above and general numerical calculations is good for angles of interest. Several observations can be made concerning these equations.

- Perturbation of the circulating beam to first order in θ is a small deflection in position and angle. It is not a function of initial position or angle. There is no change in strength of the lens. There is no x-y coupling.
- Typical deflections are listed in the Table below. A correction of .042 mrad, corresponding to a magnet tilt of 20 mrad, corresponds to 0.65 A on a dipole trim.

Table 1
Beam deflection due to tilting quadrupole D4Q5

D4Q5 tilt, $\Delta\theta$	$\Delta y(\ell)$	$\Delta y'(\ell)$
0	0	0
10 mrad	.16 mm	.021 mrad
20 mrad	.32 mm	.042 mrad

- Deflection is up for a defocusing lens tilted upward (as in the sketch); down for a defocusing lens tilted downward. The deflection of the injected beam will also be reduced by this amount, but the change is negligible.

General orbits.

In general the orbit of a particle beam will not follow exactly the standard paraxial equations above even in a perfect quadrupole. The bending force depends on the cross product between the local particle direction and the magnetic field. The effect is to change the strength of the magnet to

$$\sqrt{\kappa} = \left(B' \cos\theta / B\rho\right)^{1/2}$$

where θ is the angle between the local beam trajectory and the magnetic field direction. In addition the effective length of the magnet increases by the factor $\cos\theta$. Based on these corrections, one can calculate a simple numerical model to estimate the corrections to the standard equations as a function of angle θ. These corrections are relevant to both the injected beam, which enters the magnet at an angle of over 60 mrad, and the circulating beam, which enters at an angle of up to 16 mrad as the magnet is tilted. They are listed in the table below as the differences in the terms in the quadrupole deflection equation between the simple equations and the numerical model. The notation $y|y_0$ represents the dependence of final deflection y on initial y, etc.

Table 2
Large-angle corrections to the quadrupole deflection terms

$\Delta\theta$	$y\|y_0$, $y'\|y_0'$	$y\|y_0'$	$y'\|y_0$
0	0	0	0
10 mrad	-5.23×10^{-6}	-5.18×10^{-5}	-1.84×10^{-6}
20	-2.09×10^{-5}	-2.07×10^{-4}	-7.37×10^{-6}
40	-8.32×10^{-5}	-8.30×10^{-4}	-2.935×10^{-5}
60	-1.88×10^{-4}	-1.87×10^{-3}	-6.61×10^{-5}

The optical aberration that the circulating beam undergoes due to corrections of less than 0.02% is small. The injected beam undergoes much larger aberrations, but still not dangerous for a single pass. Similar corrections occur in the opposite plane.

A more accurate result may be obtainable by directly integrating the equations of motion through the quadrupole. Also a complete list of second order terms for the ideal quadrupole can be found for example in Ref.[3].

Wei-shi Wan has done a tracking study for the Debuncher, to look for nonlinear effects on the circulating beam of tilting D4Q5 15 and 30 mrad, using COSY. His results show that the effects of a 15-mrad tilt are negligible. For a 30-mrad tilt, some particles are lost at large radius. The minimum effective aperture is 5 times larger than the radius of 40 π beam after 100000 turns. The strongest effect is for off-momentum particles. There is no noticeable effect on the tunes. Since the proposed tilt is at most 16 mrad, the tilted quad should have no significant effect on Debuncher performance.

Injection septum.

The injection septum has been a source of some confusion. The calibration for the deflection of the septum, based on measurements with reverse protons, is quoted in Ref. 1 as 32.8 mrad. But, as also noted in the same report, there is a serious discrepancy between the bend angle produced by such a deflection on reverse protons, and the geometrical requirement for keeping the beam centered inside the beam pipe through the AP2 line quadrupoles. In particular the exit aperture of IQ33 is at a measured height of 461.2 mm at a measured distance of 4.749 m from the upstream end of D4Q5. In order to remain centered in the beam pipe, the vertical angle of the reverse proton beam between D4Q5 and IQ33 must be 65.3 mrad. A septum deflection of 32.8 mrad yields a vertical angle of only 58.9 mrad, based on the beam model below, and the beam is off center at IQ 33 by 43 mm. This discrepancy is too large to overlook. Centering the beam in the beam line

requires a septum deflection of 36.6 mrad. An error or uncertainty of ±0.6 mrad in septum calibration (only ±1.7%) corresponds to missing the beampipe center at IQ33 by ±6 mm.

The pulsed current monitor for the septum power supply is a B-dot coil that was initially calibrated against a Pearson current monitor, but may have drifted over time. For accuracy it is necessary to calculate the operating current. I modeled the septum field using POISSON, based on the dimensions of the laminations and the known positions of the conductors [Ref. 4]. The prediction from POISSON is that the current required to develop a bend field of 6.0 kG is 19.0 kA. This is in reasonable agreement with the design [Ref. 5], which lists a current of about 20 kA for 6 kG field. The magnet inductance from the POISSON calculation is 1.665 μH/m, or L=3.436 μH for conductor length=81.25". The septum is pulse driven by SCR discharge of a capacitor bank of capacitance C=4.78 mF charged to 650 V. The pulse length is 480 μs (from the scope photo taped outside the D:ISEP power supply). The estimate for circuit resistance is taken from Ref. 1, R=9.6 mΩ, where I have added an additional 1 mΩ for the dynamic resistance of the SCRs and connections. For these conditions the inferred inductance of the complete circuit becomes 4.77 μH. These numbers yield a current waveform that peaks at 16.36 kA at t=220 μs, and that has a pulse shape similar to that seen in the photo. Thus the septum deflecting field is 5166 Gauss, and the deflection angle is 36.0 mrad, assuming the effective length of the septum is the same as length of the conductor. This amount of deflection suggests quadrupole steering of roughly 6 mm in the AP2 line. There are uncertainties in this calculation, particularly because the circuit resistance is not well known. But the consistency between the geometrical and POISSON calibrations of the septum is encouraging. A value of 36.0 mrad deflection is used for the existing optics case below.

The cause for the apparently low deflection angle produced by the experimental septum calibration of Ref. 1 is not clear. One possibility is that the circulating reverse proton beam may have not been well centered in the Debuncher aperture during the measurement. Measurements made under these circumstances could be in error depending on the local position and angle of the circulating beam. Forcing agreement in the optics model between the 32.8 mrad deflection and the geometrical requirements requires offsetting the circulating beam well off axis, and passing the injected beam outside the good field region of D4Q5.

The injection septum is an aperture limitation in both planes. The vertical septum gap is too large - 15.4 mm, and the horizontal aperture is too small - 39 mm.

D4Q4.

The injected beam passes through D4Q4 well off axis, centered at about 58 mm above the Debuncher centerline. Figure 4 shows the field gradient (quadrupole component) calculated by POISSON for large distance from the axis using the laminations for a small quad. It shows that the top of the star chamber, which was apparently extended upward from its original location at some time in the past, is located at the upper edge of the good field region (80.5 mm). At present the injected beam scrapes at this location. Thus the beam should be redirected downward in this region in order to avoid this limitation. The vacuum chamber at the upstream and downstream locations may be extended upward a few mm before reaching the good-field limit.

D4Q3.

The injected beam is about 16 mm off axis at D4Q3. This quadrupole also plays a role in deflecting the injected beam before it reaches the kicker, but no problems are expected here.

The solutions described below require some vertical displacement of this quadrupole, in order to better center it on the circulating beam, which is to be deflected downward through the injection region.

Injection kicker.

There is some uncertainty in the calibration of the injection kicker. The optimal vertical aperture through the injection region is obtained in the optics model for a deflection of 5.89 mrad. This prediction depends sensitively on the position of the circulating beam, and correct geometrical placement of the vacuum chamber walls in the relevant locations. The design deflection of the kicker is 6.1 mrad, and experimental calibration is about 6.34 mrad. Geometrical considerations are not nearly as strong in this case as in the case of the septum; an uncertainty of this magnitude in kicker deflection angle (less than ±0.3 mrad) translates into a position uncertainty of a few mm or less. To be conservative, a deflection of only 5.89 mrad was assumed in the model for current operation, increasing to a deflection of 6.4 mrad for the first solution. Larger deflections and larger vertical aperture would be attainable if these numbers prove to be too pessimistic.

The aperture of the elliptically-shaped vacuum chamber in the kicker is adequate for both the circulating and injected beam.

Beam optics model.

Using the MAD model of the Debuncher, known values for trim dipole settings in the injection region, and vertical BPM data provided by Mike Church, I generated a spreadsheet model of the vertical motion of the beam through the injection region. The model uses the standard matrix model for particle motion using Courant-Snyder parameters through a lattice. This model has been verified by an independent model that geometrically calculates positions based on deflections generated by the beamline elements.

Fig. 5 shows 40π beam in the central injection region (gray with dots - circulating beam, gray with open triangles - injected beam) and the vacuum chamber walls (thick solid lines). The injected beam is scraping on D4Q4 and on the septum. The top of the injected beam scrapes at D4Q4, and the bottom of the injected beam scrapes at the septum. The vertical aperture is optimized when these two losses are equal. If the kicker is turned up, for example, losses at D4Q4 become much worse. The horizontal aperture is tightest at the large quad D4Q5, and is also limited at the septum.

The vertical centroid location is shown in fig. 6. The curve marked 'as-is' is a least-square fit to the BPM data (solid circles). Debuncher survey data provided by Elvin Harms (fig. 7) were used to place magnet vertical offsets throughout this region. Use of the measured offsets, referenced to the average elevation in the injection region, improves comparisons between model and BPM data. The other two curves represent the two solutions described below.

The available apertures of the existing injection region estimated from the optics model are 26 π mm mrad horizontal and 21 π mm mrad vertical. These estimates are needed to design the aperture upgrade. They are considerably larger than experimentally measured apertures for injected beam. These aperture measurements tend to be in the range of 15 π in each plane. The discrepancy could be due to one or more causes.

One possibility is dispersion. For example, dispersion measurements provided by Jim Morgan using reverse protons show that the horizontal dispersion at SEM 733 is not zero, but about 0.13 m. If the dispersion is also 0.13 m at D4Q5, a 2% off-momentum particle has a displacement of 2.6 mm. The horizontal beta function at the center of D4Q5 is 17.83, and the horizontal beam pipe half width is 21.4 mm. Thus an off-momentum particle has a nominal acceptance of less than 20 π. The only place in the injection region where the vertical dispersion has a clear effect on aperture is in the septum - D4Q4 region. The vertical dispersion in this area is 0.04 - 0.06 m, according to P138. The effect is to raise or lower the injected beam by up to 1.2 mm for 2% off-momentum particles, reducing vertical aperture for off-momentum particles to about 18 π.

Some other possibilities are:
- Uncertainties in beam and vacuum chamber locations in the model
- Dispersion mismatch and mistuning of the beta functions through the tight spots
- Distortions of the magnetic field in D4Q5 at extreme vertical offsets
- Aperture restrictions elsewhere in the beamline
- Mis-steered beam

Proposed modifications.

Solutions to beam transport for increased aperture were designed to match the end points of the beam for the base-line condition. Two solutions to the aperture upgrade are described here. Extensive use was made of Excel's constrained optimization routine 'Solver'. Longitudinal motion of D4Q5 was modeled based on a MAD run with D4Q5 displaced 12 cm downstream. This magnet move changes the beta functions throughout the Debuncher by as much as 0.54 m.

Solution 1 is designed to open up the vertical and horizontal apertures to the limits of the existing septum, with minimal perturbation to the circulating beam, and modest requirements on the injection kicker. The position of D4Q5 is offset downstream by 6 cm. Vertical aperture can be as large as 33 π with the injection kicker at 6.4 mrad. The solution deflects the beam downward through the D4Q4 bottleneck by using the trims and corrects by a vertical offset of D4Q5, which is advantageous for horizontal aperture. The solution is constrained to keep quadrupole steering of the circulating beam less than 4 mm, and trim dipole settings at less than half their rated currents of 25 A. Vertical beam sizes and locations with respect to the vacuum chamber wall are indicated in fig. 8. The locations of the centroids of the respective circulating beams are shown in fig. 6.

Horizontal aperture is improved by two factors.
1. The flat vacuum chamber for injected beam is replaced with a triangular-shaped chamber that better fits D4Q5's pole shape in the region of the injected beam. Horizontal aperture is increased at all vertical locations except the top of the beam. Quoted aperture is for the vertical centroid of the beam.
2. The magnet D4Q5 is raised by 3.1 mm, moved downstream by 6 cm, and tilted to face AP2 by 8 mrad. The effect is to lower the height of the injected beam along the pole face from 150 mm to 140 mm. In this location the horizontal aperture is wider, and perhaps equally important, the injected beam is moved away from the poorly-documented extreme edge region of the quadrupole field.

Solution 2 is similar to Solution 1, but the magnet moves are larger, to provide further increases in aperture. Quadrupole steering of the circulating beam is allowed up to 6 mm, and trim magnet settings are allowed up to 18 A. Aperture is opened up by moving D4Q5 downstream by the full 12 cm, upward by 8.60 mm at the midplane, and tilted by 16 mrad.

At a pole-face height of 127 mm, the horizontal aperture is 40 π. It is necessary to move the septum upstream by 30 cm and increase its strength to provide sufficient bend to the injected beam. Beam sizes are shown in fig. 9 through the central injection region. The entire injection region is shown (for Solution 2) in fig. 10 Photographs of the principal optical elements in the injection region are shown in Figures 11 through 14.

Changes are summarized in the table below. The assumption is that the existing septum will limit horizontal aperture in the first case to 31 π, and that a new septum will be produced for the second case with a 40 π horizontal aperture. If the vertical septum gap is reduced by at least 1 mm, and if a deflection at the kicker of 6.6 mrad can be obtained, the vertical aperture will also be 40 π. Until the new septum is on hand, Solution 1 is preferred, because of the relatively modest changes required. Sketches of the vacuum chamber requirements through the large quad D4Q5 are shown in Figures 15 and 16.

The spreadsheets used to generate the three cases are attached to the back of this report. They are labeled 'as is', '6 cm', and '12 cm'.

Table 3.
Baseline conditions and model predictions for the solutions studied.

	Baseline (as-is)	**Solution 1**	**Solution 2**
V401 curr.	+1.4 A	-11.2 A	-18.1 A
IKIK defl.	5.89 mrad	6.4 mrad	6.6 mrad
V403 curr.	-2.8 A	+9.12 A	+16 A
D4Q3 pos. (vert.)	--	+2.74 mm	-0.78 mm
D4Q4 d.s. (pipe)	--	+4 mm	+4 mm
ISEP d.s. (vert)	--	-8.3 mm	-6.3 mm
ISEP u.s. (vert)	--	-6 mm	-6 mm
ISEP pos. (long)	--	--	-30.0 cm
ISEP defl.	36.0 mrad	35.8 mrad	37.9 mrad
D4Q5 pos. (vert.)	--	+3.10 mm	+8.62 mm
D4Q5 pos. (long.)	--	+6.0 cm	+12 cm
D4Q5 tilt	--	-8 mrad	-16 mrad
V406 curr.	-2.6 A	-11.8 A	-5.44 A
D4Q8 defl.	--	--	+0.245 mrad
height on pole face	148.3 mm	139.8 mm	126.9 mm
Ax [mm mrad]	26 π	31 π	40 π
Ay [mm mrad]	21 π	33 π	40 π

New Injection Septum.

The new injection septum should have a horizontal aperture of 47 mm to accommodate the increased horizontal beta function at the upstream end of the septum (13.8 m) and a 40-π horizontal aperture at its new location. The effective length and the gap height should stay the same, assuming the septum is designed with curvature. The number of RG-220 cables supplying the current should be increased from 4 to 6, and the number of capacitors in the power supply should be increased from 5 to 6. With these changes the pulse length and charge voltage for the new septum/power supply remain very similar to the existing power supply. Parameters calculated from a simple model are listed in the table below. The septum should be as thin as possible - no more than 12 mm, preferably 11 mm.

Table 4.
Parameters of septum and power supply

	existing septum	new septum
gap width	39.7 mm	47.0 mm
gap height	53 mm	53 mm
length of laminations	80"	80"
septum inductance	3.44 μH	2.92 μH
# of cables	4	6
circuit inductance	4.77 μH	3.89 μH
circuit resistance	9.57 mΩ	7.21 mΩ
# of capacitors	5	6
capacitance	4.78 mF	5.74 mF
pulse length	480 μsec	474 μsec
voltage	650 V	655 V
peak current	16.36 kA	20.3 kA
magnetic field	5.17 kG	5.44 kG
beam deflection	36.0 mrad	37.9 mrad

Work to be done.

1. The beam calculations should be verified with a computer model such as TRANSPORT that is entirely independent of the MAD output.
2. Design of a new septum for full horizontal aperture should proceed, based on the parameters in Table 4. Modifications should be made to the power supply as noted, and the current monitor calibration should be checked.
3. Solution 2 should be re-evaluated in light of the results of Solution 1 after they are determined experimentally and compared with these predictions.

References.

1. M. Church, Recent AP2 studies and a proposal to increase the transverse aperture to 40 pi mm mrad, dated 10/6/97
2. M. Gormley, S. O'Day, An updated AP2 beamline TURTLE model, Pbar Note 510 (5/23/91).
3. K.L. Brown, A first and second order matrix theory for the design of beam transport systems and charged particle spectrometers, SLAC 75 (June 1982).
4. L.W. Oleksiuk, Design study of the TeV I pulsed septum magnet, Fermilab TM-1241 (Feb. 1984).
5. J.A. Satti and S.D. Holmes, A pulsed septum magnet for the Fermilab Antiproton Source, IEEE Trans. Nucl. Sci. NS-32, 3628 (1985).

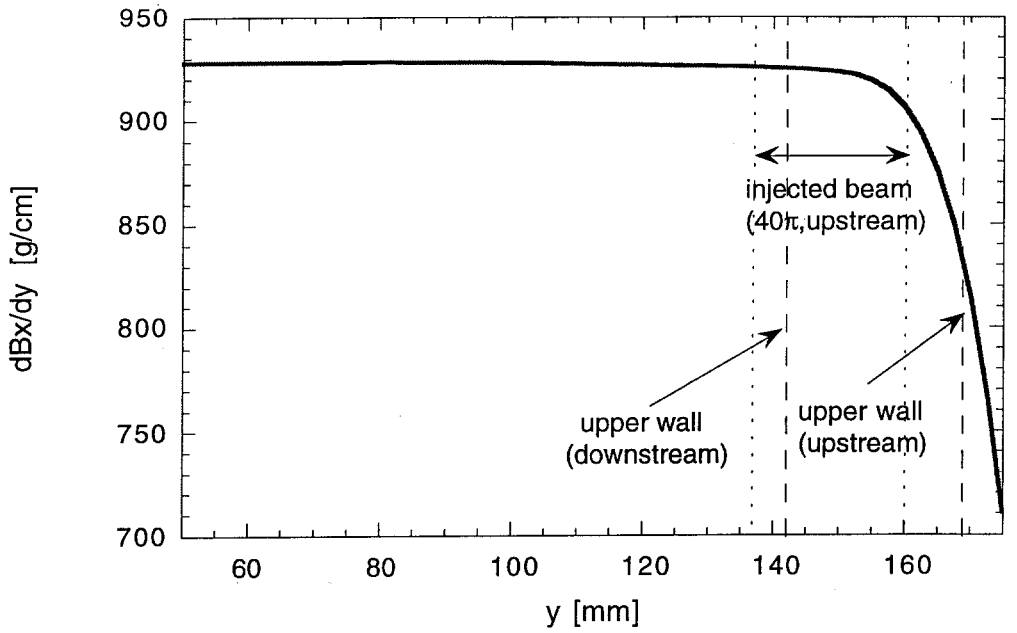

Figure 1. Field gradient for large vertical position in D4Q5 at nominal field strength. Shown are current position of the injected beam at upstream end of the magnet, and current positions of the upper beam pipe wall.

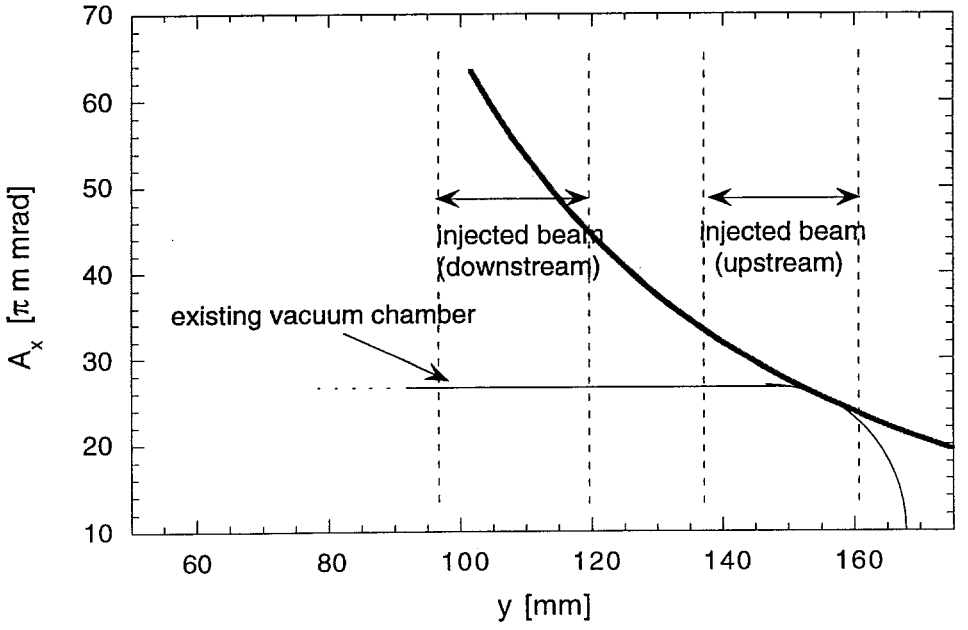

Figure 2. Horizontal aperture of D4Q5 available between pole faces. Indicated are current positions of the injected beam at the upstream and downstream locations, and the effective aperture of the existing vacuum chamber.

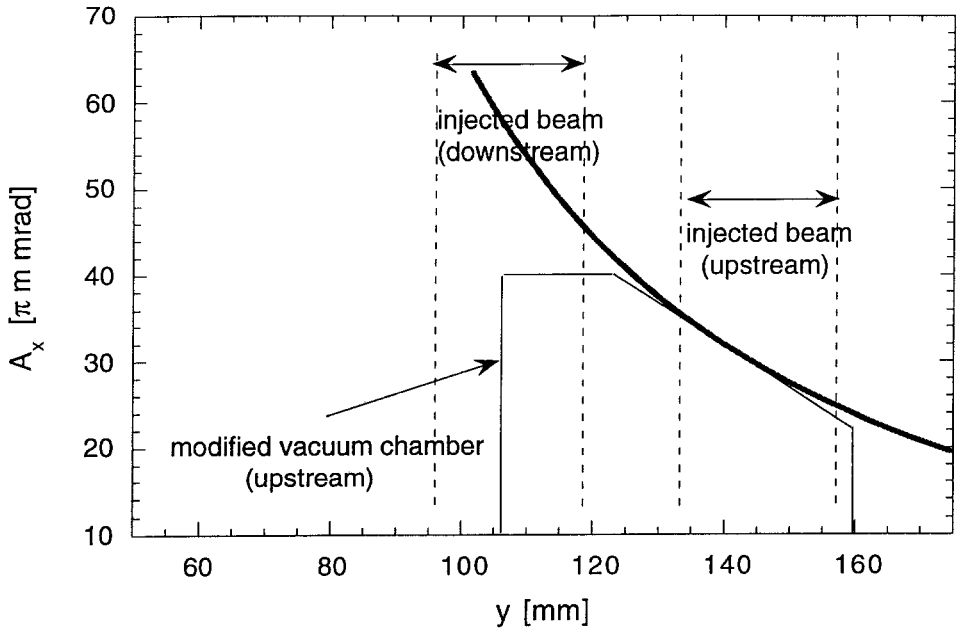

Figure 3. Horizontal aperture of D4Q5 with a modified vacuum chamber.

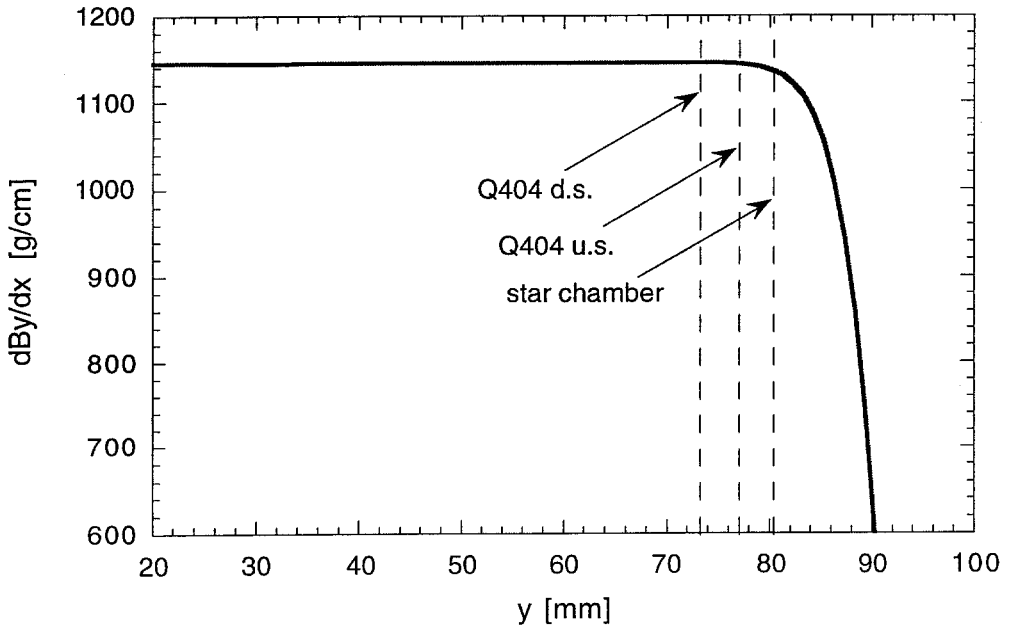

Figure 4. Field gradient for large vertical position in D4Q4 at nominal field strength. Shown are the positions of the upper beam pipe wall at three locations: downstream, upstream, and in the star chamber.

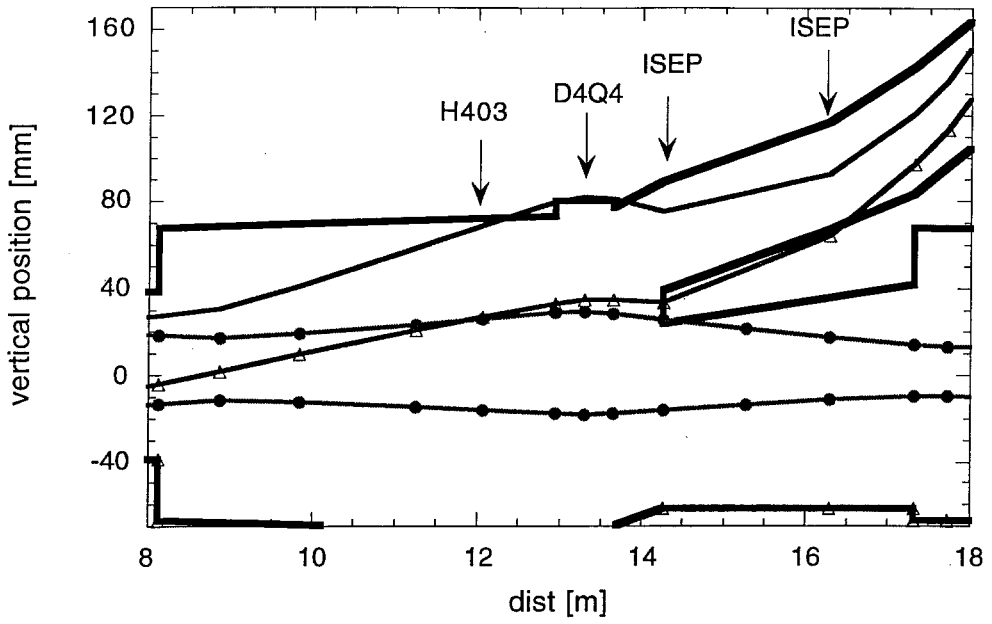

Figure 5. Vertical beam positions and sizes for existing configuration of injection region. Shown are the vacuum wall locations and beam size for a 40-π beam.

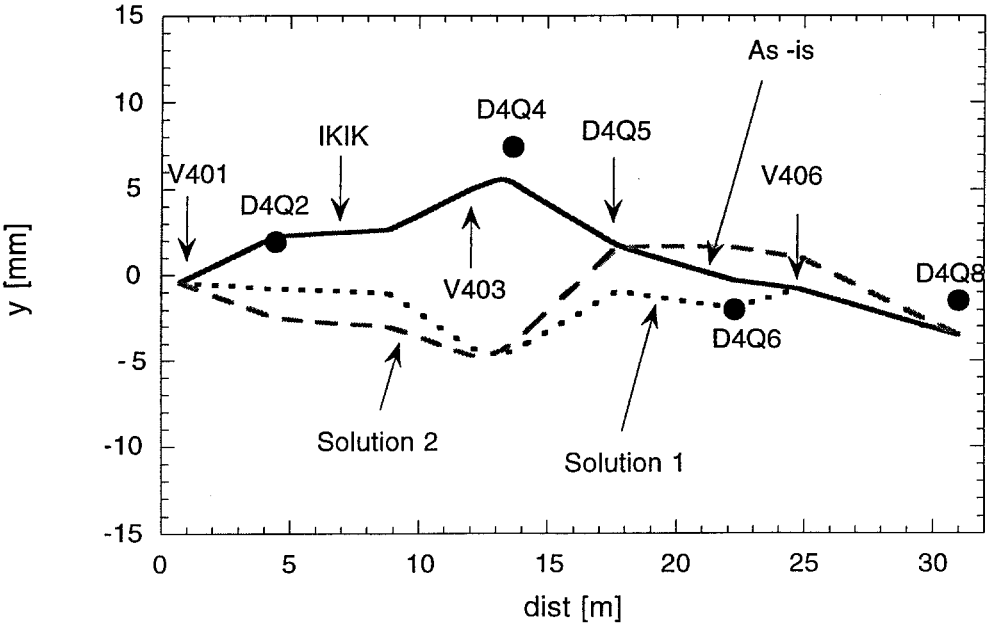

Figure 6. Centroid locations for existing circulating beam, Solution 1, and Solution 2. Also shown are BPM data used to locate the existing beam vertical positions.

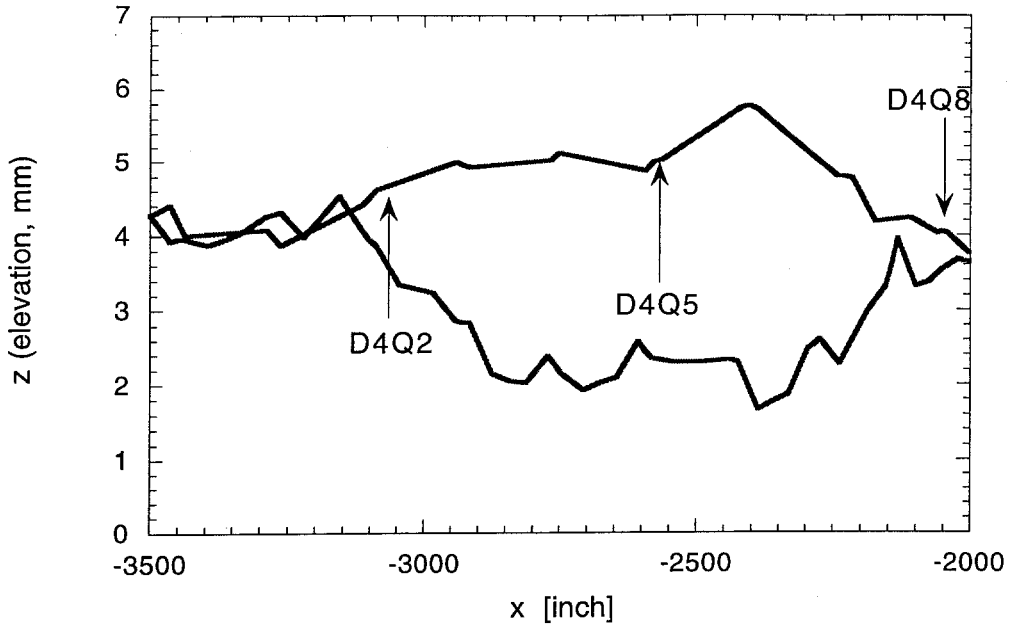

Figure 7. Debuncher survey elevations near the injection region.

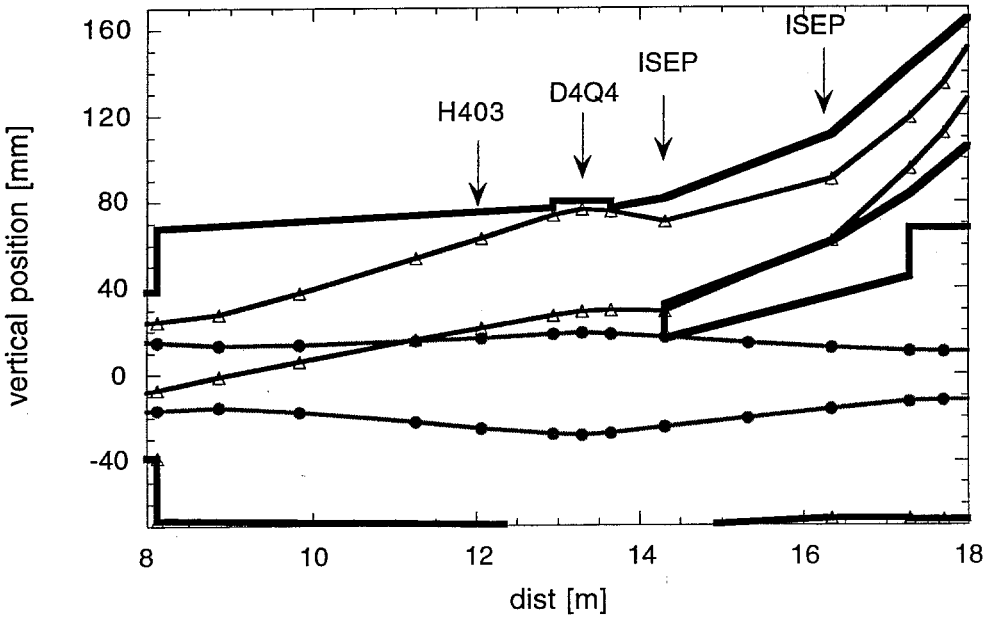

Figure 8. Vertical beam positions and sizes for Solution 1 in the center of the injection region. Shown are the modified vacuum wall locations and beam size for a 40-π beam.

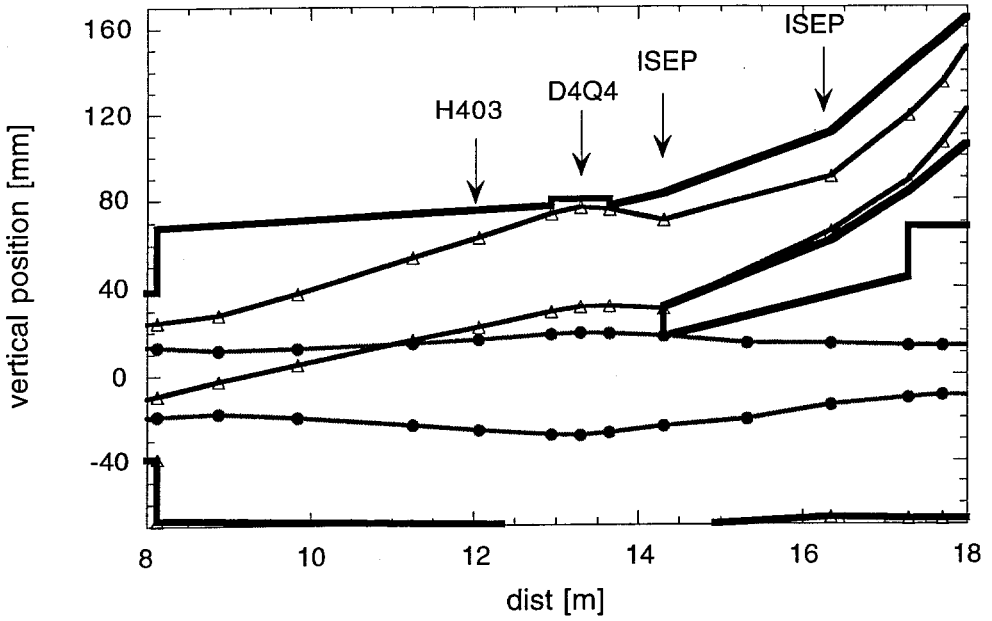

Figure 9. Vertical beam sizes and positions for Solution 2. Shown are the modified vacuum wall locations and beam size for a 40-π beam.

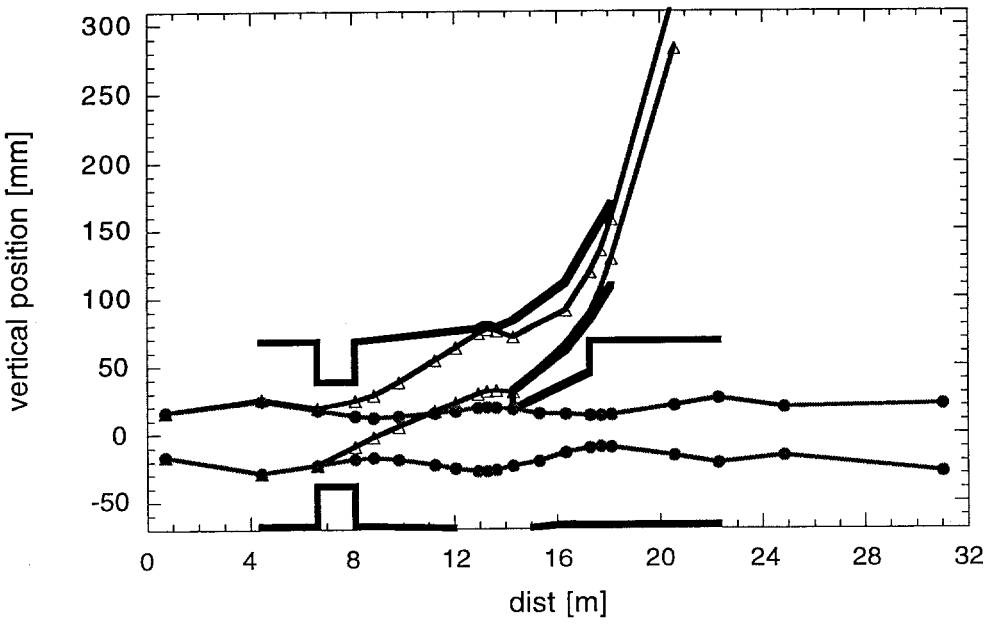

Figure 10. Vertical beam sizes and positions throughout the injection region for Solution 2.

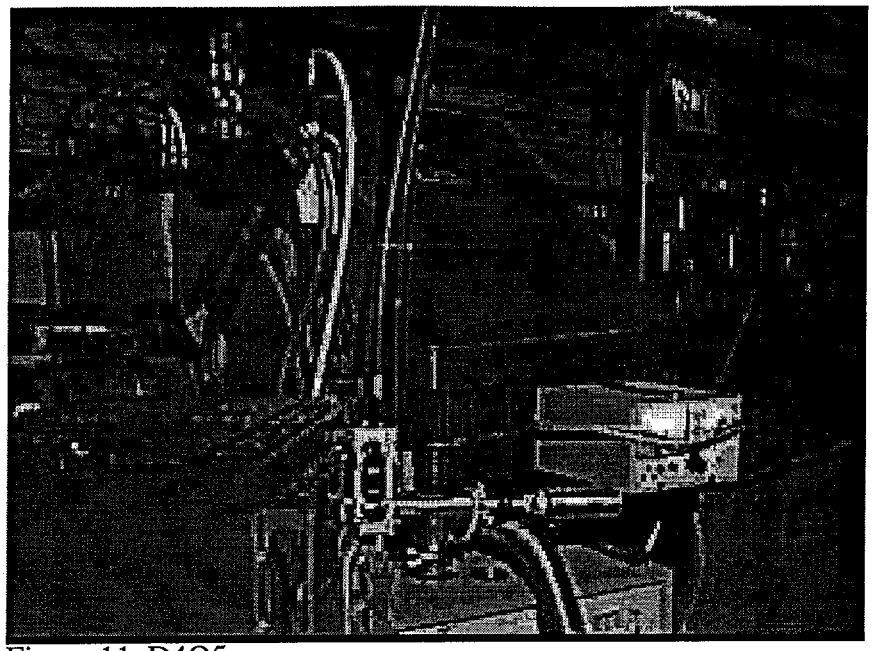

Figure 11. D4Q5.

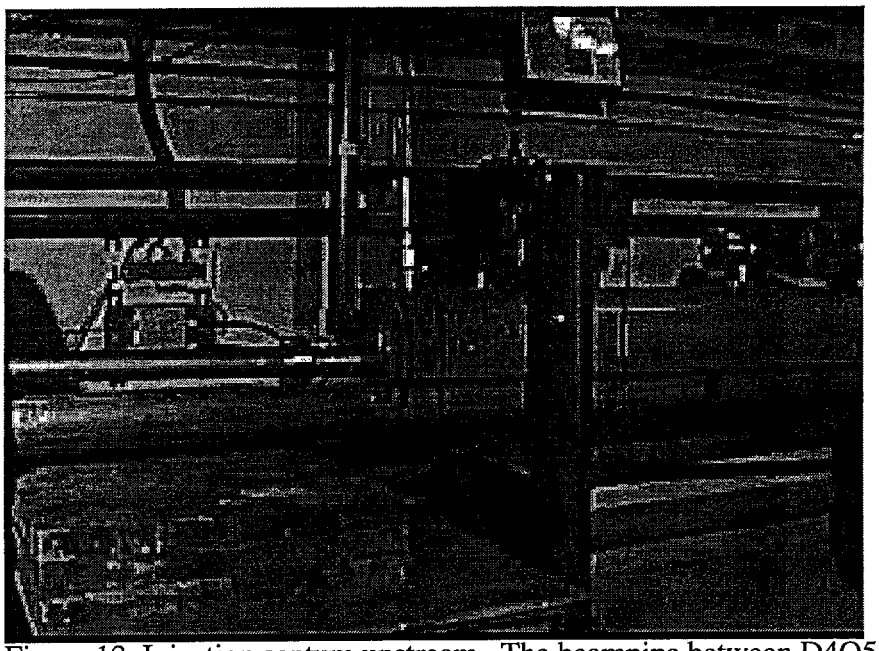

Figure 12. Injection septum upstream. The beampipe between D4Q5 and the injection septum is completely surrounded by a pile of shielding bricks (not shown in photo).

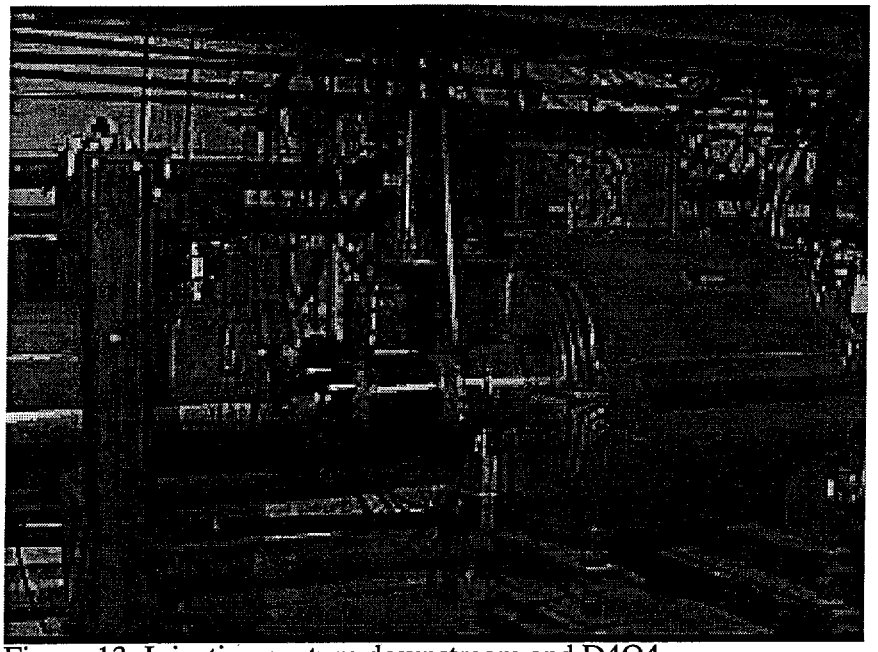

Figure 13. Injection septum downstream and D4Q4.

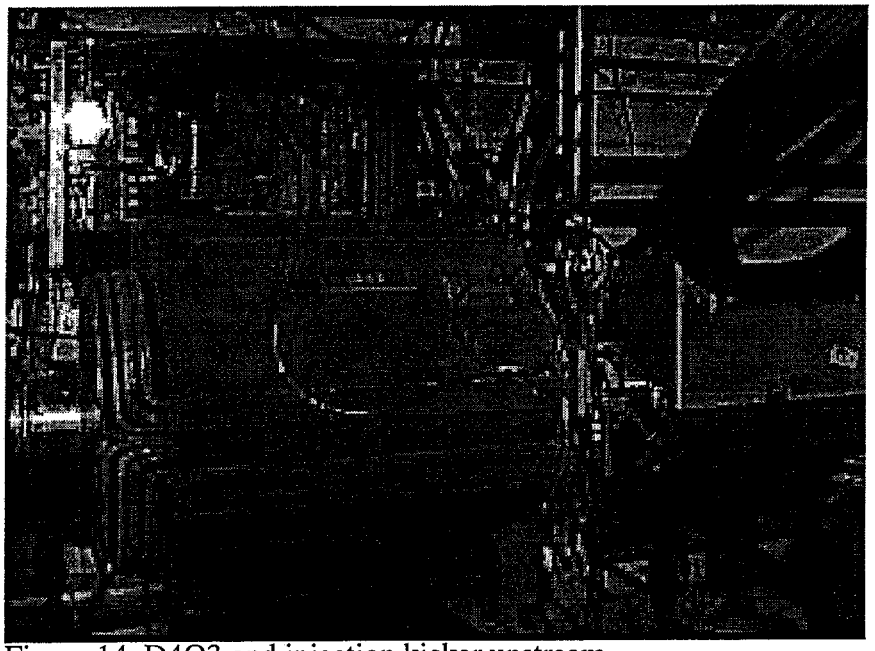

Figure 14. D4Q3 and injection kicker upstream.

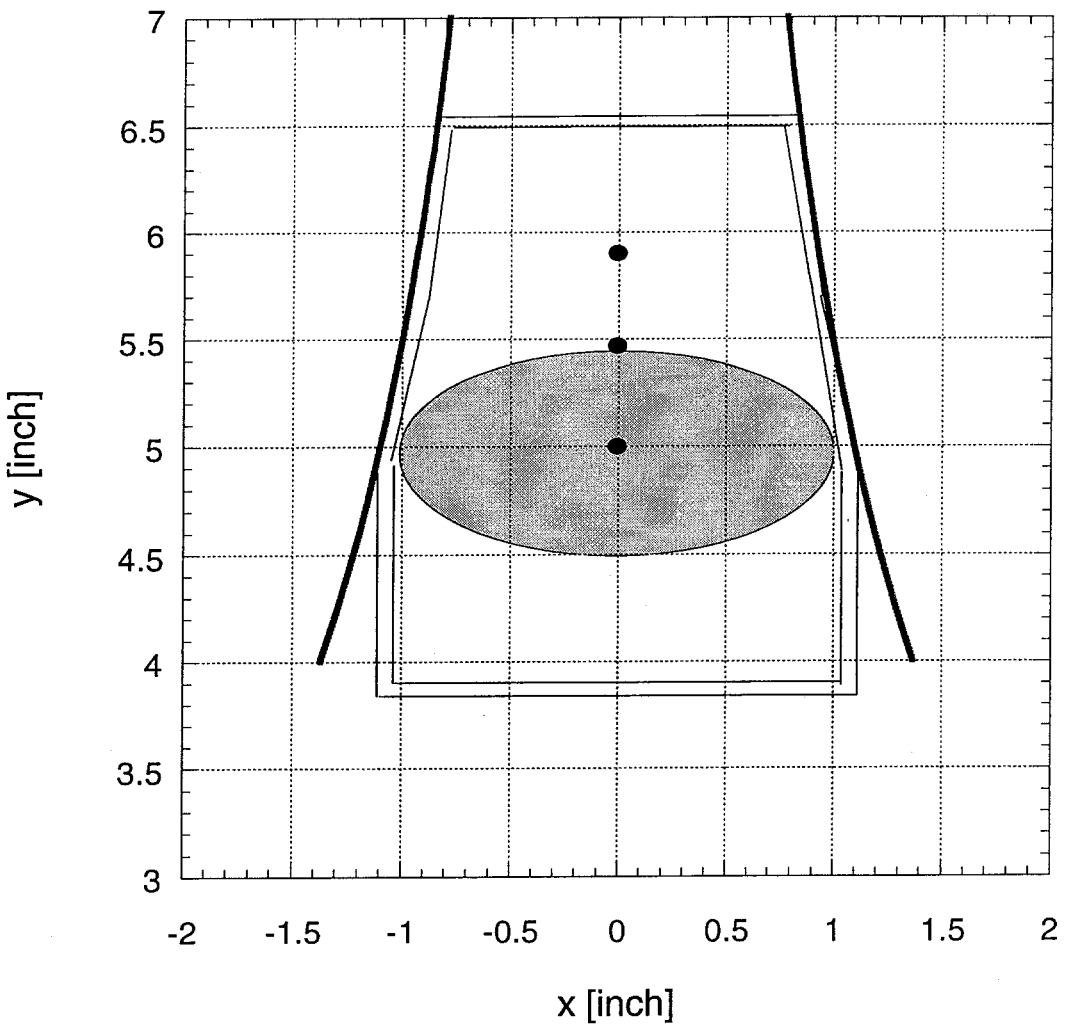

Figure 15. D4Q5 upstream vacuum chamber for injected beam. The curved lines represent the magnet laminations. Dimensions are with respect to the lamination. The solid dots represent the central beam locations for the existing conditions (upper), solution 1 (middle), and solution 2 (lower). The filled ellipse represents the approximate 40 π emittance beam size. The horizontal inside width of the rectangular portion of the pipe must be at least 2.11". The vacuum chamber is cut off at 6.5" (165 mm) because the field quality of the magnet is poor above this height.

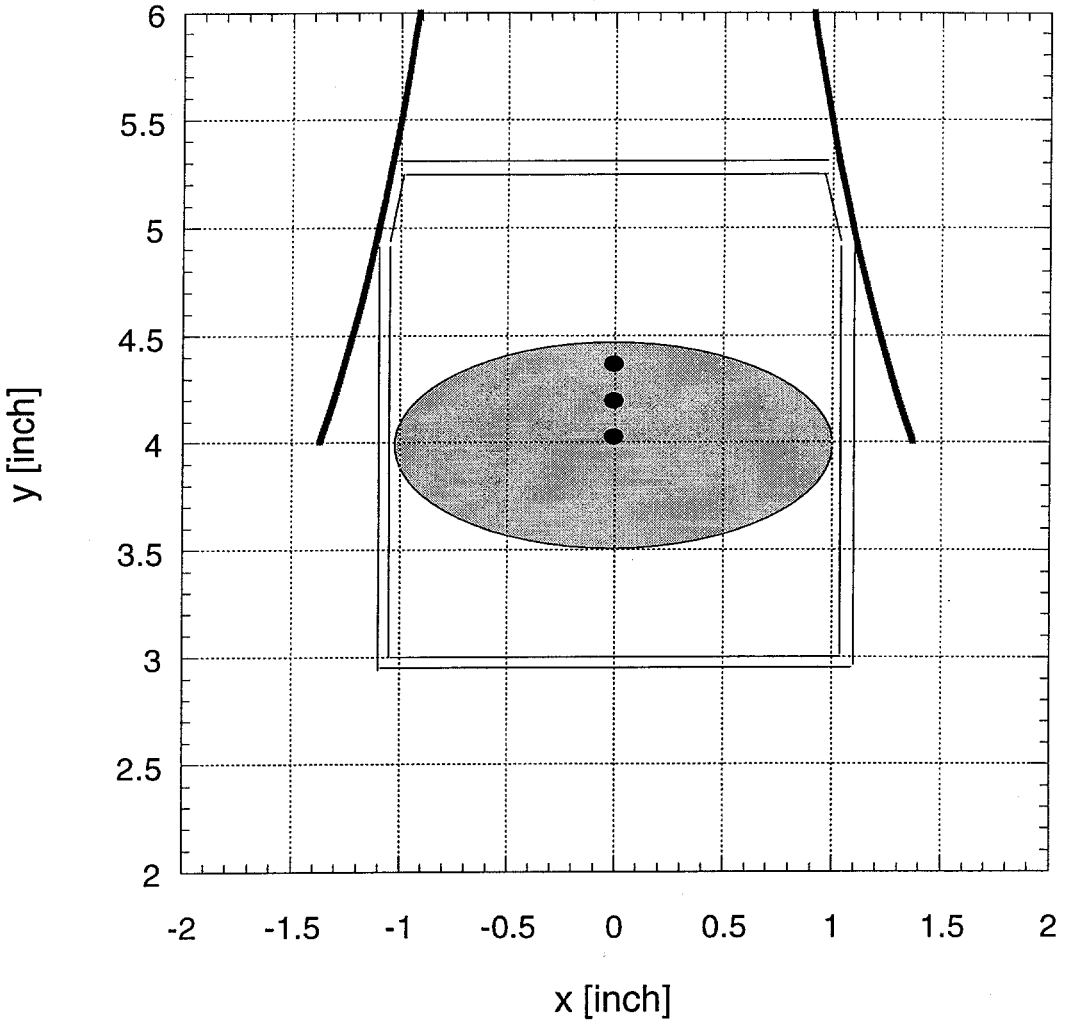

Figure 16. D4Q5 downstream vacuum chamber and injected beam locations.

updated 6/9/98, new septum calibration														
			Injected beam as-is											
element	z [mm]	beta-y	alpha-y	psi-y	kick	angle	position				vertical	vert. aper.		
					(mr)	(mr)	(mm)				limit (mm)	mm-mrad		
Q402 cent		16.98	0.051	0.471	-0.1398	0.339	2.24							
IKIK cent		9.747	1.444	0.641	5.89	5.952	2.424	optimum at 5.89 mrad						
IKK ds		6.177	0.977	0.836	0	5.919	11.37				38.4	118.27		
Q403 cent		5.129	0.108	0.968	0.032	7.825	15.99							
H403 cent		6.171	-0.779	1.144	0	10.02	25.3							
SEM 403		8.909	-1.149	1.338	0	10.03	39.62							
V403 cent		10.94	-1.36	1.42	-0.189	9.837	47.72	<< -2.801 A , .0674 mrad/A						
Q404 ds		13.54	-1.589	1.489	0	9.831	56.24				73.1	20.989		
Q404 cent		14.02	0.249	1.514	0.0139	2.049	58.33				80.2	34.14		
Q404 us		13.2	2.041	1.546	0	-5.908	57.89				77.2	28.233	(was 74 mm - vacuur	
ISEP ds		10.85	1.802	1.596	8.2	2.3	54.26				39.1	21.169	88.9	110.579
ISEP cent		7.599	1.405	1.703	20.2	22.63	56.09							
ISEP us		5.15	1.007	1.866	8.2	30.82	79.14				67	28.602	116.8	275.443
Q405 ds		3.492	0.605	2.111	0	30.81	110.8				83.3	217.28		
Q405 cent		3.239	0.018	2.237	0.0138	46.7	127				96.2	292.77		
Q405 us		3.461	-0.564	2.362		65.21	150.1				109.1	486.44		
SEM 733		8.422	-1.486	2.827	0	65.22	308							
SEM 733	2.42					65.22	308					20.989	min apt	
Q 733 ds	4.749					65.22	459.8	<- measured ht=461.2 mm						
			Circulating beam as-is											
element		beta-y	alpha-y	psi-y	kick (mra	angle (n	position (mm)							
							calc		meas.	delta-y				
						0.647	-0.459	min. rms deviations						
V401 cent		6.523	-0.952	0.119	0.095	0.742	-0.459	<- + 1.412A (.0674 mrad/A)						
Q402 cent		16.98	0.051	0.471	-0.1398	0.339	2.24	-0.559	1.92	0.32	<- guess on calibration of offset			
IKIK cent		9.747	1.444	0.641	0	0.062	2.424							
IKK ds		6.177	0.977	0.836	0	0.059	2.525				38.4	208.36		

Q403 cent		5.129	0.108	0.968	0.032	0.416	2.62	-0.127	.2519	mrad/mm				
H403 cent		6.171	-0.779	1.144	0	0.757	3.294							
SEM 403		8.909	-1.149	1.338	0	0.757	4.373							
V403 cent		10.94	-1.36	1.42	-0.189	0.568	4.985							
Q404 ds		13.54	-1.589	1.489	0	0.57	5.489				73.1	337.64		
Q404 cent		14.02	0.249	1.514	0.0139	-0.168	5.557	0.051	.2723	mrad/mm	80.2	397.51		
Q404 us		13.2	2.041	1.546	0	-0.913	5.361		7.44	-2.079	70.8	324.39		
ISEP ds		10.85	1.802	1.596	0	-0.913	4.804				23.7	32.9		
ISEP cent		7.599	1.405	1.703	0	-0.912	3.885							
ISEP us		5.15	1.007	1.866	0	-0.912	2.959				35.7	208.15		
Q405 ds		3.492	0.605	2.111	0	-0.912	2.021				67.7	1235.3		
Q405 cent		3.239	0.018	2.237	0.0138	-0.649	1.695	-0.051			67.7	1345.1		
Q405 us		3.461	-0.564	2.362	0	-0.438	1.469				67.7	1267.4		
SEM 733		8.422	-1.486	2.827	0	-0.438	0.408							
Q406 cent		13.89	-0.242	2.985	0.1715	-0.233	-0.345	0.686	-2.01	1.665	<-- guess on calibration of offset			
V406 cent		7.868	1.005	3.223	-0.176	-0.357	-0.814	<--2.613 A						
Q407 cent		5.341	-0.065	3.506	0.216	-0.304	-1.478	-0.864			<-- guess on calibration of offset			
Q408 cent		15.9	-0.016	4.002	0	-0.073	-3.499	0	-1.52	-1.979				
												32.9	min apt	
									8.09	3.333	root sum of squares of deviations from data			

5/19/1998 corrected sign of Q403. 6/9/98 new septum calibration													
Moving septum, Q405, bumping around										0.008	Q405 pitch angle [rad]		
		Injected beam								0	<- downstream displacement of ISE		
										6	<- downstream displacement of Q4		
										6	<- additional quad steering at Q73		
element	beta-y	alpha-y	psi-y	kick	angle	position				offset	vertical	vert. aper.	
				(mr)	(mr)	(mm)					limit (mm)	mm-mrad	
Q402 cent	17.26	0.048	0.46	-0.14	-0.15	-0.851							
IKIK cent	9.914	1.47	0.63	6.4	6.36	-0.965							
IKK ds	6.272	1	0.82	0	6.357	8.432					38.4	143.201	
Q403 cent	5.195	0.121	0.96	-0.658	7.224	13.39							
H403 cent	6.221	-0.77	1.13	0	9.077	21.8							
SEM 403	8.925	-1.134	1.32	0	9.083	34.82							upper ylim
V403 cent	10.93	-1.342	1.4	0.6146	9.697	42.16							
Q404 ds	13.49	-1.567	1.47	0	9.688	50.52				4	77.1	52.3499	
Q404 cent	13.96	0.265	1.5	0.0139	2.679	52.68				0	80.2	54.2415	good field e
Q404 us	13.13	2.047	1.53	0	-4.5	52.5				0	77.2	46.4675	
ISEP ds	10.78	1.806	1.58	8	3.475	49.83				-8.3	30.8	33.5882	80.6
ISEP cent	7.524	1.405	1.69	19.809	23.36	53.06							
ISEP us	5.08	1.003	1.85	8	31.45	76.46				-6	61	47.0517	110.8
Q405 ds	3.508	0.621	2.09		31.38	107.1					83.3	161.509	
Q405 cent	3.243	0.032	2.21	-0.828	45.91	123.4					96.2	228.879	
Q405 us	3.453	-0.55	2.34		63.95	146.1					109.1	397.343	
SEM 733	8.496	-1.485	2.81		63.98	304.6							
SEM 733	2.48				63.98	304.8							
Q 733 ds	4.809				63.98	453.8	<- measured ht=461.2 mm						
					goal is angle=65.22,pos=459.8 @Q 733 us							33.5882	min apt
								3.6E-05	<-sum of squares of deviation of endpoints from as-is				
		Circulating beam						348.068	<-sum of squares of trim currents				
								139.75	<- height of beam on Q405 pole face				
element	beta-y	alpha-y	psi-y	kick	angle	posit. (mm)		quad cal.	initial				
				(mr)	(mr)	calc	I-trim	mrad/mm	quad offsets				
					0.647	-0.46							
V401 cent	6.589	-0.976	0.12	-0.757	-0.11	-0.46	-11.23	<- amps in trim					
Q402 cent	17.26	0.048	0.46	-0.14	-0.15	-0.851	0	0.25	-0.559				
IKIK cent	9.914	1.47	0.63	0	-0.04	-0.965							
IKK ds	6.272	1	0.82	0	-0.04	-1.024					38.4	222.745	

Q403 cent	5.195	0.121	0.96	-0.658	-0.83	-1.077	2.738	-0.2519	-0.127				
H403 cent	6.221	-0.77	1.13	0	-0.98	-1.997							
SEM 403	8.925	-1.134	1.32	0	-0.99	-3.41							
V403 cent	10.93	-1.342	1.4	0.6146	-0.37	-4.205	9.118						
Q404 ds	13.49	-1.567	1.47	0	-0.37	-4.54					73.1	348.356	
Q404 cent	13.96	0.265	1.5	0.0139	0.261	-4.562	0	0.2723	0.051		80.2	409.893	
Q404 us	13.13	2.047	1.53	0	0.868	-4.357					70.8	336.111	
ISEP ds	10.78	1.806	1.58	0	0.868	-3.822				-8.3	15.4	34.2716	
ISEP cent	7.524	1.405	1.69	0	0.868	-2.948							
ISEP us	5.08	1.003	1.85	0	0.868	-2.071				0	35.7	280.864	
Q405 ds	3.508	0.621	2.09	0	0.868	-1.228					67.7	1259.54	
Q405 cent	3.243	0.032	2.21	-0.828	-0.1	-0.897	3.103	-0.2714	-0.051		67.7	1376.09	
Q405 us	3.453	-0.55	2.34	0	-0.23	-0.965					67.7	1289.77	
SEM 733	8.496	-1.485	2.81	0	-0.23	-1.529							
Q406 cent	13.94	-0.227	2.97	0.1715	0.194	-1.867	0	0.25	0.686				
V406 cent	7.835	1.017	3.21	-0.794	-0.36	-0.806	-11.79						
Q407 cent	5.341	-0.065	3.51	0.216	-0.3	-1.514	0	-0.25	-0.864				
Q408 cent	15.64	-0.02	4	0	-0.07	-3.5	0	0.25					
				goal is Q408 angle=-.07, Q408 position =-3.5									
												34.2716	min apt

P (cm)											
05 (based on 12 cm displaced MAD run)											
3											
		beta-nom	alpha-no	psi-non	beta-m	alpha-m	psi-mod				
		16.98	0.051	0.47	17.54	0.044	0.459				
		9.747	1.444	0.64	10.08	1.496	0.628				
		6.177	0.977	0.84	6.366	1.022	0.811				
		5.129	0.108	0.97	5.26	0.134	0.942				
		6.171	-0.779	1.14	6.271	-0.76	1.112				
upper apt		8.909	-1.149	1.34	8.941	-1.12	1.307				
		10.94	-1.36	1.42	10.92	-1.32	1.389				
		13.539	-1.589	1.49	13.45	-1.55	1.458		Corrections for moving ISEP:		
xtends to about 80.5 mm		14.016	0.249	1.51	13.9	0.28	1.483		corr beta	corr alpha	corr psi
		13.201	2.041	1.55	13.07	2.052	1.508				
87.82455		10.853	1.802	1.6	10.71	1.809	1.565		10.781	1.8055	1.58
		7.599	1.405	1.7	7.448	1.404	1.678		7.5235	1.4045	1.69
232.1612		5.15	1.007	1.87	5.009	0.999	1.841		5.0795	1.003	1.854
		3.492	0.605	2.11	3.524	0.637	2.061				
		3.239	0.018	2.24	3.247	0.046	2.187				
		3.461	-0.564	2.36	3.445	-0.54	2.312				
		8.422	-1.486	2.83	8.569	-1.48	2.796				
		6.523	-0.952	0.12	6.654	-1	0.113				
		16.98	0.051	0.47	17.54	0.044	0.459				
		9.747	1.444	0.64	10.08	1.496	0.628				
		6.177	0.977	0.84	6.366	1.022	0.811				

		5.129	0.108	0.97	5.26	0.134	0.942				
		6.171	-0.779	1.14	6.271	-0.76	1.112				
		8.909	-1.149	1.34	8.941	-1.12	1.307				
		10.94	-1.36	1.42	10.92	-1.32	1.389				
		13.539	-1.589	1.49	13.45	-1.55	1.458				
		14.016	0.249	1.51	13.9	0.28	1.483				
		13.201	2.041	1.55	13.07	2.052	1.508				
		10.853	1.802	1.6	10.71	1.809	1.565				
		7.599	1.405	1.7	7.448	1.404	1.678				
		5.15	1.007	1.87	5.009	0.999	1.841				
		3.492	0.605	2.11	3.524	0.637	2.061				
		3.239	0.018	2.24	3.247	0.046	2.187				
		3.461	-0.564	2.36	3.445	-0.54	2.312				
		8.422	-1.486	2.83	8.569	-1.48	2.796				
		13.886	-0.242	2.98	13.99	-0.21	2.953				
		7.868	1.005	3.22	7.801	1.029	3.192				
		15.9	-0.016	4	15.39	-0.02	3.99				

5/19/1998 corrected sign of Q403. 6/8/98 new septum calibration													
Moving septum, Q405, bumping around										0.016	Q405 pitch angle [rad]		
		Injected beam								-30	<- downstream displacement of ISE		
										12	<- downstream displacement of Q4		
										6	<- additional quad steering at Q73		
element	beta-y	alpha-y	psi-y	kick	angle	position				offset	vertical	vert. aper.	
				(mr)	(mr)	(mm)					limit (mm)	mm-mrad	
Q402 cent	17.54	0.044	0.46	-0.14	-0.41	-2.541							
IKIK cent	10.08	1.496	0.63	6.6	6.511	-2.833	max defl=6.81 mr @ 64.5 kV						
IKK ds	6.366	1.022	0.81	0	6.538	6.628					38.4	158.574	
Q403 cent	5.26	0.134	0.94	0.2294	8.07	11.76							
H403 cent	6.271	-0.761	1.11	0	9.73	20.77							
SEM 403	8.941	-1.119	1.31	0	9.739	34.78							upper ylim
V403 cent	10.92	-1.323	1.39	1.0784	10.82	42.65							
Q404 ds	13.45	-1.545	1.46	0	10.8	51.95				4	77.1	47.0446	
Q404 cent	13.9	0.28	1.48	0.0139	3.576	54.46				0	80.2	47.6844	good field e
Q404 us	13.07	2.052	1.51	0	-3.82	54.37				0	77.2	39.8887	
ISEP ds	10.71	1.809	1.56	8	3.812	51.22				-6.3	30.8	38.9303	82.6
ISEP cent	7.448	1.404	1.68	21.835	25.29	55.28	nom defl=32.8 mr						
ISEP us	5.009	0.999	1.84	8	32.05	80.73				-6	61	77.7308	110.8
Q405 ds	3.524	0.637	2.06	0	34.05	102					83.3	98.8009	
Q405 cent	3.247	0.046	2.19	-2.327	46.44	119.3					96.2	165.002	
Q405 us	3.445	-0.535	2.31		63.96	142.1					109.1	316.858	
SEM 733	8.569	-1.483	2.8		64.01	304.3							
SEM 733	2.54				64.01	304.7							
Q 733 ds	4.869				64.01	453.8	<- measured ht=461.2 mm						
					goal is angle=65.22,pos=459.8 @Q 733 us							38.9303	min apt
								3.6E-05	<-sum of squares of deviation of endpoints from as-is				
		Circulating beam						612.2668	<-sum of squares of trim currents				
								126.9398	<- height of beam on Q405 pole face				
element	beta-y	alpha-y	psi-y	kick	angle	posit. (mm)		quad cal.	initial				
				(mr)	(mr)	calc	I-trim	mrad/mm	quad offsets				
					0.647	-0.46							
V401 cent	6.654	-0.999	0.11	-1.218	-0.57	-0.46	-18.08	<- amps in trim					
Q402 cent	17.54	0.044	0.46	-0.14	-0.41	-2.541		0.25	-0.559				
IKIK cent	10.08	1.496	0.63	0	-0.09	-2.833							

IKK ds	6.366	1.022	0.81	0	-0.09	-2.953					38.4	197.374	
Q403 cent	5.26	0.134	0.94	0.2294	-0.24	-3.092	-0.784	-0.2519	-0.127				
H403 cent	6.271	-0.761	1.11	0	-0.64	-3.638							
SEM 403	8.941	-1.119	1.31	0	-0.64	-4.55							
V403 cent	10.92	-1.323	1.39	1.0784	0.44	-5.067	16						
Q404 ds	13.45	-1.545	1.46	0	0.433	-4.728					73.1	347.615	
Q404 cent	13.9	0.28	1.48	0.0139	1.072	-4.47	0	0.2723	0.051		80.2	412.624	
Q404 us	13.07	2.052	1.51	0	1.649	-4					70.8	341.463	
ISEP ds	10.71	1.809	1.56	0	1.641	-2.932				-6.3	17.4	38.6039	
ISEP cent	7.448	1.404	1.68	0	1.642	-1.275							
ISEP us	5.009	0.999	1.84	0	1.649	0.36				0	35.7	249.33	
Q405 ds	3.524	0.637	2.06	0	1.645	1.872					67.7	1373.5	
Q405 cent	3.247	0.046	2.19	-2.327	-0.38	2.623	8.623	-0.2714	-0.051		67.7	1523.05	
Q405 us	3.445	-0.535	2.31	0	-0.04	2.536					67.7	1431.94	
SEM 733	8.569	-1.483	2.8	0	-0.04	2.449							
Q406 cent	13.99	-0.211	2.95	0.1715	-0.18	2.303	0	0.25	0.686				
V406 cent	7.801	1.029	3.19	-0.366	-0.85	1.131	-5.437						
Q407 cent	5.341	-0.065	3.51	0.216	-0.65	-0.512	0	-0.25	-0.864		<-- guess on calibration of offset		
Q408 cent	15.39	-0.024	3.99	0.2452	-0.07	-3.495							
				goal is Q408 angle=-.07, Q408 position =-3.5									
												38.6039	min apt

EP (cm)											
05 (based on 12 cm displaced MAD run)											
3											
		beta-nom	alpha-no	psi-nor	beta-m	alpha-m	psi-mod				
		16.98	0.051	0.47	17.54	0.044	0.459				
		9.747	1.444	0.64	10.08	1.496	0.628				
		6.177	0.977	0.84	6.366	1.022	0.811				
		5.129	0.108	0.97	5.26	0.134	0.942				
		6.171	-0.779	1.14	6.271	-0.76	1.112				
upper apt		8.909	-1.149	1.34	8.941	-1.12	1.307				
		10.94	-1.36	1.42	10.92	-1.32	1.389				
		13.539	-1.589	1.49	13.45	-1.55	1.458		Corrections for moving ISEP:		
xtends to about 80.5 mm		14.016	0.249	1.51	13.9	0.28	1.483		corr beta	corr alpha	corr psi
		13.201	2.041	1.55	13.07	2.052	1.508				
91.961		10.853	1.802	1.6	10.71	1.809	1.565		9.6873	1.74534	1.594
		7.599	1.405	1.7	7.448	1.404	1.678		6.6447	1.36488	1.721
180.49		5.15	1.007	1.87	5.009	0.999	1.841		4.4095	0.99912	1.906
		3.492	0.605	2.11	3.524	0.637	2.061				
		3.239	0.018	2.24	3.247	0.046	2.187				
		3.461	-0.564	2.36	3.445	-0.54	2.312				
		8.422	-1.486	2.83	8.569	-1.48	2.796				
		6.523	-0.952	0.12	6.654	-1	0.113				
		16.98	0.051	0.47	17.54	0.044	0.459				
		9.747	1.444	0.64	10.08	1.496	0.628				

		6.177	0.977	0.84	6.366	1.022	0.811				
		5.129	0.108	0.97	5.26	0.134	0.942				
		6.171	-0.779	1.14	6.271	-0.76	1.112				
		8.909	-1.149	1.34	8.941	-1.12	1.307				
		10.94	-1.36	1.42	10.92	-1.32	1.389				
		13.539	-1.589	1.49	13.45	-1.55	1.458				
		14.016	0.249	1.51	13.9	0.28	1.483				
		13.201	2.041	1.55	13.07	2.052	1.508				
		10.853	1.802	1.6	10.71	1.809	1.565				
		7.599	1.405	1.7	7.448	1.404	1.678				
		5.15	1.007	1.87	5.009	0.999	1.841				
		3.492	0.605	2.11	3.524	0.637	2.061				
		3.239	0.018	2.24	3.247	0.046	2.187				
		3.461	-0.564	2.36	3.445	-0.54	2.312				
		8.422	-1.486	2.83	8.569	-1.48	2.796				
		13.886	-0.242	2.98	13.99	-0.21	2.953				
		7.868	1.005	3.22	7.801	1.029	3.192				
		15.9	-0.016	4	15.39	-0.02	3.99				